DRAFT
(9/13/76

OPERATION AND CONTROL OF HIGH DENSITY TOKAMAK REACTORS*

CONF-760935-22

S. E. Attenberger and D. G. McAlees+
Oak Ridge National Laboratory, Oak Ridge, Tennessee 37830

MASTER

NOTICE
This report was prepared as an account of work sponsored by the United States Government. Neither the United States nor the United States Energy Research and Development Administration, nor any of their employees, nor any of their contractors, subcontractors, or their employees, makes any warranty, express or implied, or assumes any legal liability or responsibility for the accuracy, completeness or usefulness of any information, apparatus, product or process disclosed, or represents that its use would not infringe privately owned rights.

I. INTRODUCTION

The power density produced in a reactor plasma depends on the density and temperature of the fuel ions burned. In the case of a deuterium-tritium fueled system, this quantity is given by $N_D N_T \langle\sigma v\rangle Q_F$. Tokamak reactors will have to operate under ignition conditions to attain economic viability. This requirement imposes parametric constraints on the containment system since ignition depends on density, temperature, and energy confinement time. The energy confinement time in turn depends on other variables but at present this dependence is not known. There are indications, however, that confinement time will scale favorably with an increase in density. This result is suggested both by experiments and theoretical analyses. Thus there are incentives from several points of view to operate the reactor plasma at high density.

*Research sponsored by the Energy Research and Development Administration under contract with Union Carbide Corporation.

+Exxon Nuclear Co., Inc.

By acceptance of this article, the publisher or recipient acknowledges the U.S. Government's right to retain a non-exclusive, royalty-free license in and to any copyright covering the

Several approaches for achieving high density can be envisioned. A method which requires a moderate magnetic field (or high beta) is desirable for economic reasons. This may be possible using the concept of a flux-conserving tokamak.[1] Noncircular plasmas may offer a means to high density.[2] Finally, high magnetic fields (or low beta) may be necessary.[3] In this paper a reference system which includes a moderate magnetic field, a moderately elongated plasma and high beta has been assumed.

High density imposes constraints on the design and operation of the system. For example, high power density means that the first wall will be subjected to high neutron fluxes (> 1 MW/m^2) as well as a high thermal flux. The breakdown and current rise phases of start-up may require high voltages when increased filling pressures are used. Supplemental heating using neutral beams may be difficult due to the beam energies required to achieve adequate beam particle penetration. Finally, impurity and burn product effects in a dense plasma must be examined. In some cases technological developments may be needed to meet the criteria set while in other cases operating procedures may provide the desired solutions.

Specific areas affected by high density operation are discussed below. These include scaling, plasma dynamics, impurity criteria, neutral beam heating, and low density start-up.

II. SYSTEM MODELING

There are many ways to simulate the detailed energy balance processes in a tokamak. In the present work the same model used previously in the ORNL Experimental Power Reactor Design Study[4] has been adopted and the impact of high density has been assessed. The time dependent model includes deuterium, tritium, alpha, electron and impurity particle and energy balance equations. It also includes beam-plasma fusion and heating, and cold neutrals to simulate both recycling and fueling, and the effects of impurities on radiation and transport. Psuedoclassical, neoclassical, and dissipative trapped particle mode scaling laws are included. Conduction and convection times are functions of plasma collisionality.

Impurities affect plasma energetics through the creation of a fuel ion defect and by increasing Z_{EFF} and enhancing radiation losses. The source of high-Z (iron) and low-Z (carbon) impurities is due to sputtering of the wall by

deuterons, tritons, alphas, and impurities as well as by charge-exchanged neutrals and neutrons produced in the plasma. The impurity model is discussed further later.

Figure 1 shows the plasma radius required for ignition as a function of temperature. The density is 2×10^{20} m^{-3}, the plasma elongation (height to width ratio) is 1.6, and the axis magnetic field for three cases is shown. The minimum size for ignition occurs at about T = 13 keV. Below this temperature the $N\tau$ required for ignition increases sharply and an increase in size is necessary to attain it. Above 13 keV, trapped ion mode transport ($N\tau \propto \beta^2 T^{-11/2}$) dominates the scaling and an increase in plasma size again is required. The neutron wall loadings associated with various operating temperatures are also shown. Note that at $N = 2 \times 10^{20}$ m^{-3}, T = 13 keV and B_T = 45 kG, the wall loading exceeds 3 MW/m^2 and the plasma radius necessary for ignition is 1.25 m. With a field strength of 65 kG, the size required is reduced to $\sim$ 1 m and the wall loading is $\sim$ 2.5 MW/m^2.

Figure 2 shows the plasma radius required for ignition as a function of density. In these cases T = 13 keV. At lower densities the collisionality o the plasma is such that transport is dominated by the trapped ion mode which requires an increased plasma size. As density is increased the size required for ignition decreases since the impact of the trapped ion mode becomes less pronounced. There is no quantitative answer to the question of what maximum density is acceptable. Also, theoretical work[5] suggests that $\beta \sim 20\%$ or higher may be attainable. For this analysis an operating density of about 2×10^{20} m^{-3} is assumed. This results in a $\beta \sim 10\%$ at 13 keV, a wall loading less than 4 MW/m^2 and an ignition size of 1.25 m. Table 1 summarizes the reference system parameters computed from a time-dependent, self-consistent simulation model.

Table 1. Reference Parameters

Major radius, R_0(m)	5
Horizontal minor radius, a(m)	1.25
Elongation, b/a (-)	1.6
Toroidal field at winding, B_{max}(J)	8
Toroidal field on axis, B_T(T)	4.32
Plasma current, I(MA)	4
Electron density, N_e(m^{-3})	2.2×10^{20}
Ion density, N_i(m^{-3})	2.0×10^{20}

Table 1. (cont'd)

Ion temperature, T_i(keV)	13.5
Energy confinement time, τ_E(s)	1.2
Toroidal beta, β (-)	0.14
Average neutron wall loading, L_w(MW/m^2)	3.7
Thermal fusion power, P_{th} (MW)	1510

III. OPERATING CONDITIONS AND DYNAMICS

The operating parameters shown in Table 1 represent steady-state conditions. Since the model used includes the trapped ion mode where $\tau_E \propto T^{-11/2}$, the temperature increases to the point where the energy loss rate equals the heating rate due to thermonuclear alpha particles and a steady-state is achieved. Figure 3 shows $N\tau$ vs. T_e for three different values of magnetic field. $Z_{EFF} = 1$ and the system size is that given in the table. As the temperature increases, $N\tau$ is dominated by pseudoclassical, trapped electron mode, and trapped ion mode diffusion losses.[6] $N\tau$ required for ignition is also shown. For example, when $B_1 = 43$ kG ignition occurs at 10 keV, a thermal excursion occurs after ignition since P(alpha) and P(loss), and steady-state conditions are reached at 15 keV, i.e., $N\tau)_{operation} = N\tau)_{ignition}$. There is a minimum field for this size device which can provide ignition. It is about 40 kG and results in an $N\tau)_{operation}$ curve which is tangent to $N\tau)_{ignition}$. Note that this would occur at about 13 keV and 2×10^{20} m^{-3} which in turn implies a fusion power output of 1200 MW. This is an important point since it means that (assuming this scaling model) the minimum power output associated with an ignited device of this size is greater than 1000 MW. A heat removal capability compatible with this power would have to be installed in such a device.

The device could be operated at a higher field. In the 60 kG case, ignition occurs at 7 keV but the thermal excursion persists to a temperature greater than 20 keV. This is the result of improved confinement at the higher field. Under these conditions the system could achieve ignition at a density less than 2×10^{20} m^{-3}. The power produced is proportional to N^2 so that ignition conditions would be compatible with a power less than 500 MW. This, of course, represents a low beta system and is less attractive economically. Alternatively, a smaller size system could be used to achieve ignition under high field conditions. Figure 1 showed that a 1 m plasma radius may be sufficient. In this case the power output would be 630 MW when $N = 2 \times 10^{20}$ m^{-3} and $T_i = 12$ keV.

The ignition calculations above assumed a pure ($Z_{EFF} = 1$) plasma. When impurities are included, both the ignition requirement and the system operating characteristics change. Figure 4 shows this for the reference (Table 1) system. Iron is assumed to be the impurity. Due to enhanced radiation losses, ignition cannot be achieved above $Z_{EFF} = 1.5$. This establishes the impurity control criteria which will have to be met during the burn cycle of the device. Note also that in the trapped electron mode $N\tau \propto 1/Z_{EFF}$ and in the trapped ion mode $N\tau \propto Z_{EFF}$ so that the confinement characteristics cross over after the transition into the trapped ion mode.

IV. IMPURITY CONTROL

The plasma simulation model includes treatment of losses from line radiation, radiative recomination, and dielectronic recombination.[7] The model used is based on theoretical calculations by Merts et al.[8] The calculation is for iron and takes into account that, depending on plasma parameters, the iron may be partially ionized in some regions of the plasma. The results are dependent on plasma electron temperature. The impurity radiation loss is found to be approximately constant below a temperature T_e^l, and again approximately constant (with reduced magnitude) above a temperature T_e^u. A linear interpolation is used to connect the two regions. This radially dependent loss process is included in the model.

The electron temperature and electron density profiles are assumed to be centrally peaked parabolic functions of r (minor radius). The widths of these profiles are fixed by the initial conditions, namely the initial values for the average temperature and density and their assumed values at the plasma edge. The profiles are then determined. The peak values are re-computed as a function of time, since the code follows the evolution of all plasma parameter averages.

The high-Z impurity density is treated similary, but the peak of the profile is allowed to occur at arbitrarily chosen radii. In particular, the impurity density may be peaked at the wall. This model allows impurities to build up at the plasma edge or at the plasma center, so that the implications of various impurity diffusion theories may be assessed.

With the above assumptions, the total radiation integral over the plasma volume is evaluated.

Figure 5 shows typical profiles for electron density, electron temperature, impurity density, and atomic radiation. For this case the impurity profile is

centered at the plasma edge.

The high-temperature region, the transition region, and the low-temperature region can be distinguished between r = 0 and r = a. The remainder of the shape is due to the volume element variation with r and the density distributions used.

The equations used for the impurity radiation loss are:

$$P\ (w/m^3) = C\ (T_e) \times 10^{-32}\ N_e(m^{-3})\ N_{Fe}(m^{-3}), \qquad (1)$$

where

$$C\ (T_e) = 4.1 \text{ when } T_e < T_e^L$$

and

$$C\ (T_e) = 0.32 \text{ when } T_e > T_e^U\ ;$$

$$C\ (T_e) = (4.1 - 3.78)\ \frac{T_e - T_e^L}{T_e^U - T_e^L} \text{ when } T_e^L < T_e < T_e^U\ . \qquad (2)$$

For iron, T_e^L = 1.0 keV and T_e^U = 2.1 keV.

The buildup of the carbon and iron impurity densities due to sputtering from the walls is considered. The sputtering processes included in the N_C and N_{Fe} equations are due to incident particles which result from diffusion, i.e., deuterons, tritons, alphas, carbon and iron ions; fusion neutrons and neutrons incident from the blanket; fast neutral atoms from charge-exchange; and chemical sputtering of carbon. The ions that diffuse from the plasma are assumed to be monoenergetic.

Figure 6 shows the model used for sputtering by deuterons. For cases where carbon is assumed, the chemical sputtering yield[9] is taken to be constant. In the curve labeled 1 the particle sputtering yields are energy-dependent[10] and in the same ratios as those given by Behrisch[11] for Nb. The absolute values are normalized to those for deuterons (0.04). A fit to the recent sputtering data from Behrisch et al.[12] was obtained from Conn [13] and is shown for comparison.

The neutron sputtering rate is proportional to the neutron production rate in the plasma due to background and beam-plasma fusion events. The neutron sputtering coefficient is taken from Ref. (11). The result is actually for a 0.5-cm niobium wall and lithium-cooled blanket. It includes the 14.1-MeV source neutrons, and the random neutron flux at all energies which results from interactions in the blanket. The charge-exchange flux to the wall is computed from a spatial integration over the plasma. As in the radiation case above, radially dependent ion and neutral profiles are used.

The sputtering yield per unit volume is

$$\frac{1}{V} \int_V \gamma \; f\,[T(r)]\; \sigma_{CX} \frac{N_o}{4} \left({}_D N_D v_D + {}_T N_T v_T \right) dV \; ,$$

where $\gamma = \gamma_c$, or γ_{Fe} when appropriate. The neutral density is assumed to fall exponentially, as given by

$$N_o(r) = N_o(a)\; e^{-(a - r)/\lambda},$$

where λ is the characteristic length for neutral attenuation.

The sputtering coefficients, γ, are shown in Table 2.

Table 2. Peak Sputtering Yields

Carbon and Iron

Deuterons	0.04
Tritons	0.06
Alphas	0.64
Carbon	13.0
Iron	13.0
n	3.0×10^{-5}
chemical	0.03 (carbon only)

Figure 7 summarizes the technique used to incorporate sputtering and impurity effects into the plasma simulation model. Spatially averaged time-dependent parameters are computed and advanced in time in the program. As part of the calculation, spatial profiles for the plasma parameters, impurity species and neutrals in the system are assumed. The profiles are chosen to have average values consistent with those in the code. Using the spatially dependent information, charge state distributions and line and recombination radiation losses are

calculated. The results are integrated over the plasma volume and the integral results are used in the spatially independent energy balance computation. Similarly, the charge-exchange flux, which is dependent on space and energy, can be computed from the assumed profiles. This source of particle flux, together with the flux resulting from particle diffusion, is coupled to the wall by the sputtering model previously discussed. The diffusion flux is assumed to have a temperature of 100 eV. Sputtered impurities are assumed to reenter the plasma with some efficiency and on a profile which is selected a priori. It should be noted that major uncertainties exist in this area. For example, impurity transport and therefore the density profiles are not well understood; sputtering models (especially at low energies) remain to be verified; and detailed neutral behavior is an active area of concern.

It may be possible to control impurities in several ways. For the purpose of this work, two efficiencies have been defined. The first efficiency applies to the charged particle flux which is directed toward the wall, i.e., an efficiency of 90% means that only 10% of the flux impinges on the wall. This can be visualized as an unload divertor efficiency. The second efficiency applies to impurities which are returning from the wall to the plasma, i.e., a 90% efficiency means that only 10% of the sputtered impurities return into the plasma volume. This can be visualized as a screening divertor efficiency. Thus charged particle sputtering is affected by both whereas neutral sputtering is only affected by the "screening" efficiency. In the cases discussed below both efficiencies are taken to be equal so that a 99% charged particle efficiency implies a 90% neutral particle efficiency. In all cases the characteristic fall off distance for the background neutral density is taken to be 5 cm. The neutral density at the boundary is specified.

Figure 8 shows the ion temperature vs. time for the reference system and four charged particle efficiencies. The impurity is assumed to be iron and the neutral density at the boundary is assumed to be 1×10^8 cm^{-3}. The desirable pulse length is defined to be 30 seconds. For chargped particle efficiencies of 99, 95 and 90%, ignition occurs in 8 – 10 seconds using 75 MW of neutral beam injection. The burn conditions attained are essentially the same in all three cases and the 30 second cycle is achieved. When the efficiency is reduced to 80% a steady burn is not achieved. Impurity buildup causes the energy loss rate to exceed the alpha power input and the ignition condition cannot be maintained without intermittent beam heating. The limits

for beam control have been set in a manner which facilitates demonstrating the concept of beam driven operation. Beam heating is initiated whenever $T_i \leq 10$ keV and terminated when $P_\alpha - P_{loss} \geq 5$ MW. Each subsequent ignition point occurs at successively greater temperatures due to the continuous buildup of impurities and the associated increase in losses. $Z_{EFF} \approx 1.4$ during beam driven operation and igntion can be achieved but with little margin. Figure 4 showed that at about $Z_{EFF} = 1.5$ ignition cannot be achieved under the reference conditions. In fact if this mode of operation is required it must be optimized. A wide band for beam control, such as the one shown, results in minimum amount of time that the beams are on but results in large power output fluctuations. A narrow control band would have the opposite effect.

Ignition can be achieved but no maintained for 30 seconds when the charged particle efficiency is 99% and the neutral density at the plasma boundary is assumed to be 1×10^9 cm^{-3}. Sputtering due to charge exchange is excessive. Using 75 MW of neutral beam injection results in ignition after 11.5 seconds. The plasma is barely ignited however since $Z_{EFF} = 1.5$, $N = 2.2 \times 10^{20}$ m^{-3} and $T_i = 12.2$ keV. Ignition cannot be maintained and after 14.2 seconds the temperature has decayed to 10 keV and Z_{EFF} has increased to 1.63. Beam injection is initiated again but the plasma cannot be reignited due to the high impurity level. In the same system impurity control efficiencies less than $\sim$ 95% do not permit ignition at all.

The ignition requirement places requirements on the degree of impurity control which is needed and establishes the level for the neutral density in the plasma which can be tolerated. The two criteria, of course, are closely coupled.

V. HEATING AND START-UP

The fundamental aspects of neutral beam heating during the plasma start-up are discussed in this section. The supplemental heating power level necessary to achieve ignition in the reference system is about 6 seconds is found to be 75 Mw. This calculation is based on energy balance considerations using the final density ($\sim 2 \times 10^{20}$ m^{-3}) and does not include the problems of beam penetration into a dense plasma. High density and high impurity content make penetration into a large plasma increasingly difficult. Beam focussing, perpendicular injection and high beam energies may be necessary to overcome

the penetration problem. Small radius start-up and low density start-up may provide another means to solve the problem. Here the concept of low density start-up, which has previously been suggested[14,15] is outined.

Beam deposition can be characterized by the function H(r) which was first introduced by Rome et al.[16]. H(r) is a geometric measure of the deposited fast ion number density profile which results from injection. It is desirable to have the beam deposition peaked in the central region of the plasma for maximum heatin efficiency. In these calculations a deuteron beam, 30 cm in diameter, is assumed to be injected into a $Z_{EFF} = 1$ plasma.

Figure 9 shows the deposition profiles for several different beam energies. In these cases injection is nearly perpendicular (16° from perpendicular to prevent ripple trapping of the fast ions) and the density profile is assumed to be $N = 3 \times 10^{20}\ [1 - (r/a)^2] m^{-3}$. Adequate penetration can be achieved in this way if a beam energy of $\sim$ 250 keV can be made available. Impurity effects dictate an even higher energy.

High density and temperature are required at the ignition point where the beams are no longer needed to sustain the plasma energetically. It may be possible to establish the temperature conditions at low density, increase the fueling rate to build up the necessary density while continuing injection, and tolerate the less favorable injection profiles which will occur near the end of the heating phase. Figure 10 shows H(r) for 150 keV tangential injection into average densities of 7.5 10, and $20 \times 10^{19}\ m^{-3}$. The injection deposition profile is favorably peaked when $N = 7.5 \times 10^{19}\ cm^{-3}$, is relatively flat for $N = 1 \times 10^{20}\ m^{-3}$ and becomes peaked at $r/a = 0.75$ when $N = 2 \times 10^{20}\ m^{-3}$. Therefore, heating efficiency will decrease when $N > 1 \times 10^{20}\ m^{-3}$, but if this part of the heating cycle occurs over a time on the order of an energy confinement time, the less efficient heating process may well be tolerable.

Figures 10 and 11 show the time-dependent density and power histories during heating. Initially $N = 7.5 \times 10^{19}\ m^{-3}$, T = 100 eV, and $P_{beam} = 75$ MW. At t = 2 seconds, $T_i = 12$ keV and the fueling rate is increased to begin the density buildup phase. The plasma ignites and beam injection is terminated after t = 4.4 seconds. Density buildup occurs over a period of 2.4 seconds and the average energy confinement time during this phase is $\tau_E \approx 1.5$ seconds. Energetically this scenario is feasible since 75 MW is sufficient to heat the plasma to ignition at full density. In fact, more detailed studies of the approach using a coupled beam deposition-spatially dependent transport calculation is necessary to optimize the start-up procedure.

VI. SUMMARY

The incentive for high density operation of a tokamak reactor has been discussed. It is found that high density permits ignition in a relatively small, moderately elongated plasma with a moderate magnetic field strength. Under these conditions, neutron wall loadings ~ 4 MW/m^2 must be tolerated. The sensitivity analysis with respect to impurity effects shows that impurity control will most likely be necessary to achieve the desired plasma conditions. The charge exchange sputtered impurities are found to have an important effect so that maintaining a low neutral density in the plasma is critical. If it is assumed that neutral beams will be used to heat the plasma to ignition, high energy injection is required ($\sim$ 250 keV) when heating is accomplished at full density. A scenario is outlined where the ignition temperature is established at low density and then the fueling rate is increased to attain ignition. This approach may permit beams with energies being developed for use in TFTR to be successfully used to heat a high density device of the type described here to ignition.

REFERENCES

7. E. C. Crume, Jr. (ORNL), private communication, December 1975.
8. A. L. Merts, R. D. Cowan, and N. H. Magee, Jr., The Calculated Power Output from a Thin Iron-Seeded Plasma, LA-6220-MS, Los Alamos, New Mexico (1976).
9. M. I. Guseva and V. M. Gusev, Conf. on Engineering Problems of Thermonuclear Reactors, Leningrad (July 1974).
10. D. M. Meade et al., "The Effects of Impurities and Magnetic Divertors on High-Temperature Tokamaks," Plasma Physics and Controlled Nuclear Fusion Research, IAEA-CN-33/A15-4, Vol. I, p. 605, Tokyo, 1974.
11. R. Behrisch, Nucl. Fusion 12: 481 (1972).
12. R. Behrisch et al., "Measurements of the ERosion of Stainless Steel, Carbon, and SiC by Hydrogen Bombardment in the Energy Ragne of 0.5 – 7.5 keV," to be published in J. Nucl. Mater.
13. R. W. Conn (University of Wisconsin) private communication, 1975.

VII. ACKNOLEDGMENTS

The authors thank Dr. J. A. Rome for assistance in developing the beam injection portion of this work.

$\frac{1}{10} \times$ Trapped Particle

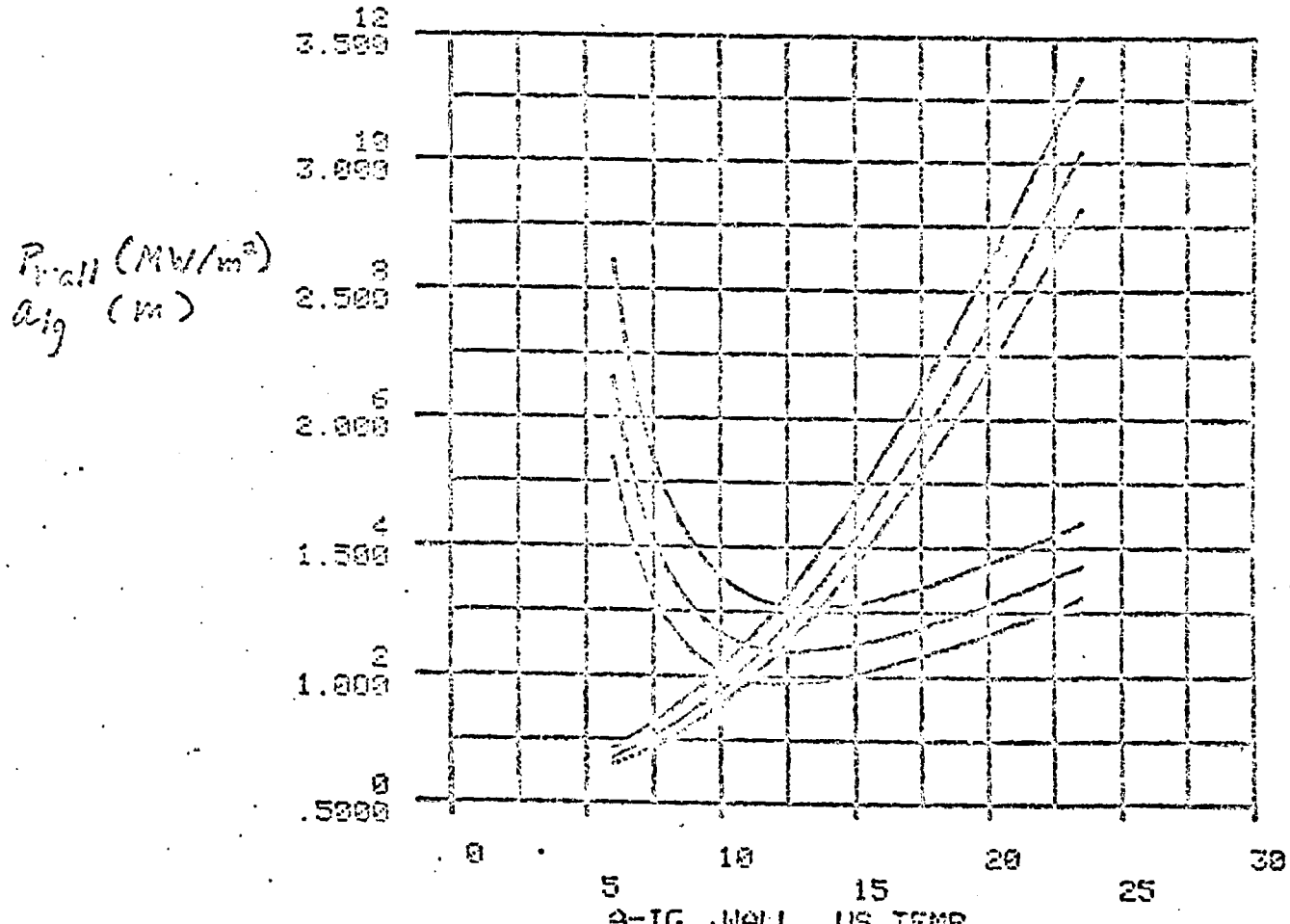

A-IG ,WALL VS TEMP
NE = 0.200E+15
CURVES OF CONSTANT BT FROM 0.450E+02 TO 0.650E+02

TWS

Figure 1

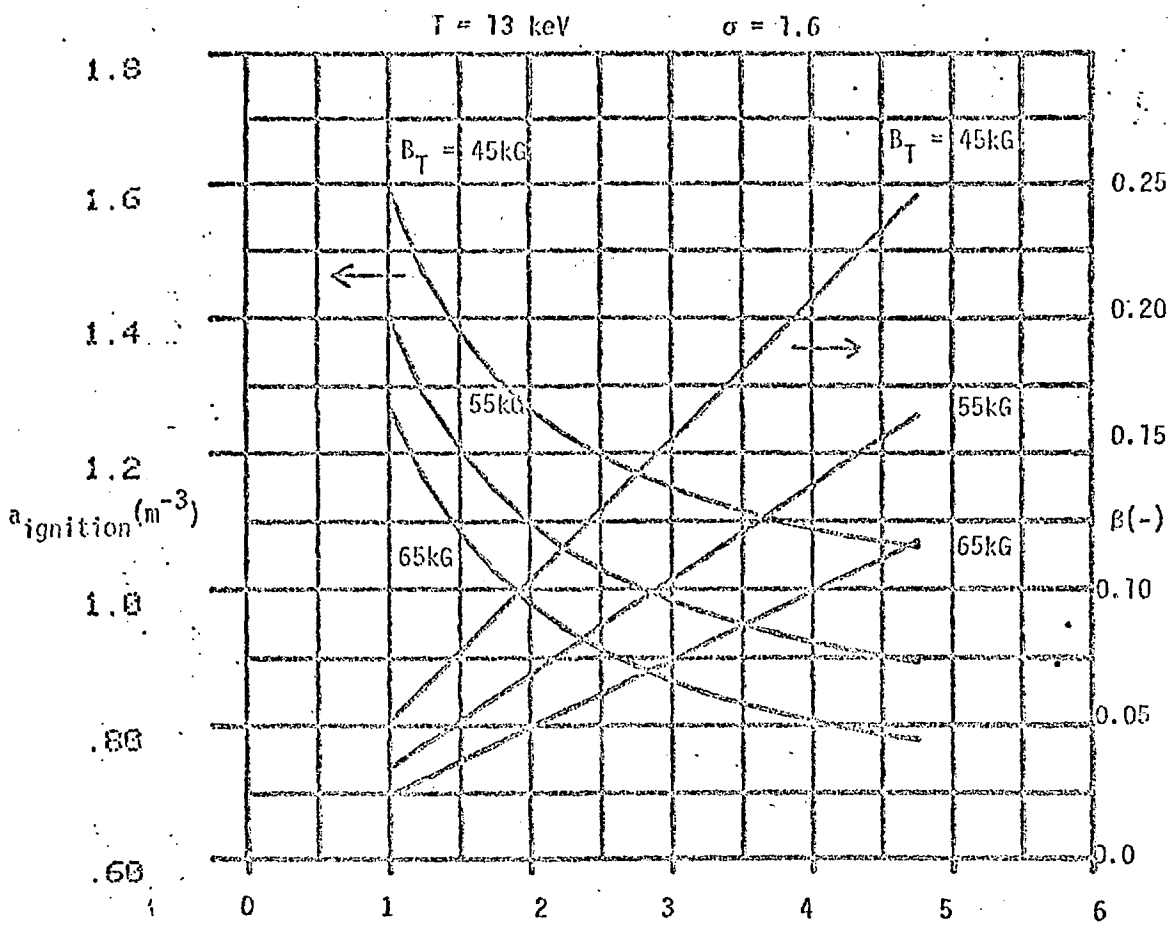

Figure 5

Figure 2

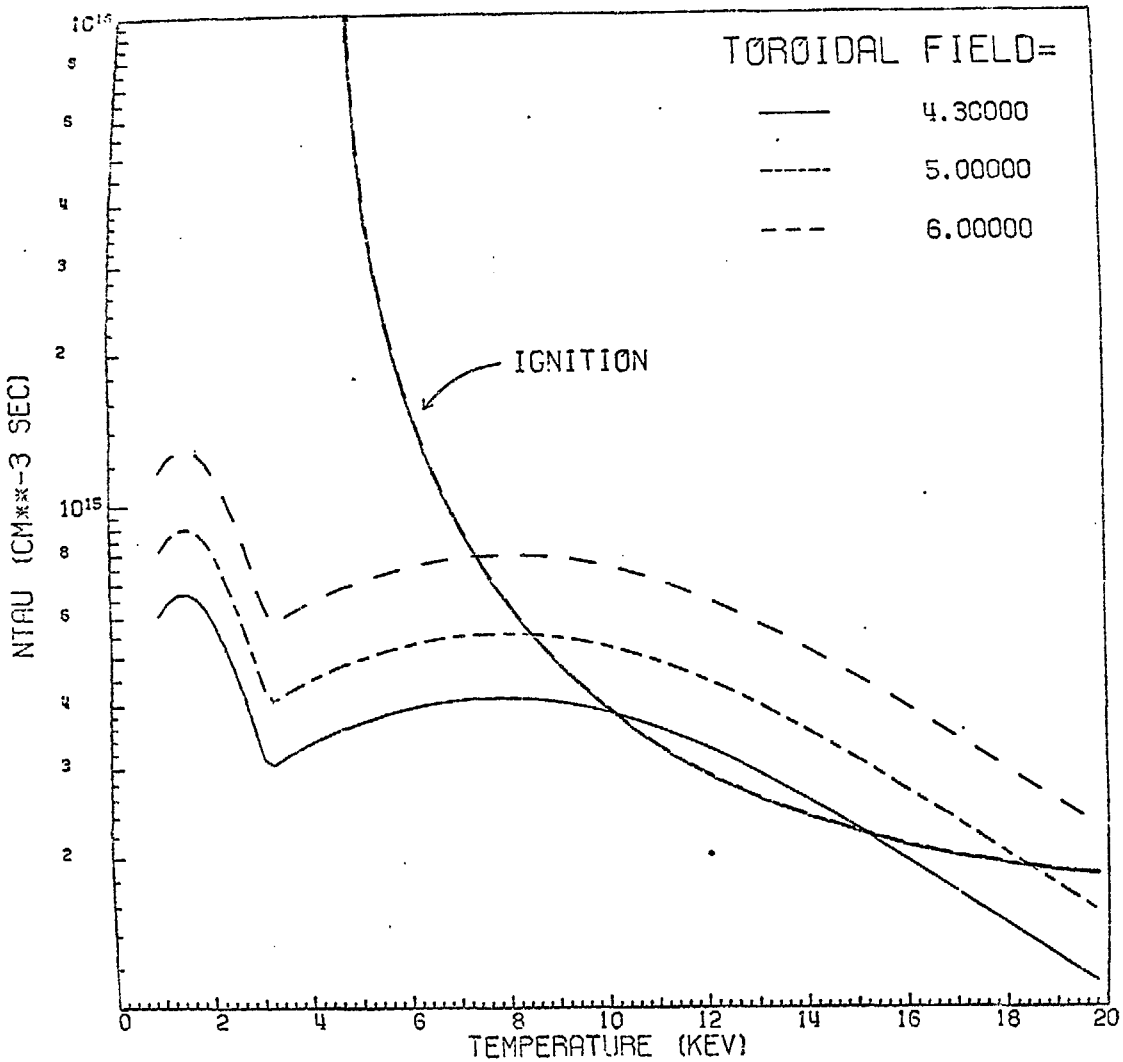
TØRØIDAL FIELD=
4.30000
5.00000
6.00000
IGNITION
NTAU (CM**-3 SEC)
TEMPERATURE (KEV)
10^15
10^15
0
2
4
6
8
10
12
14
16
18
20

Figure 3

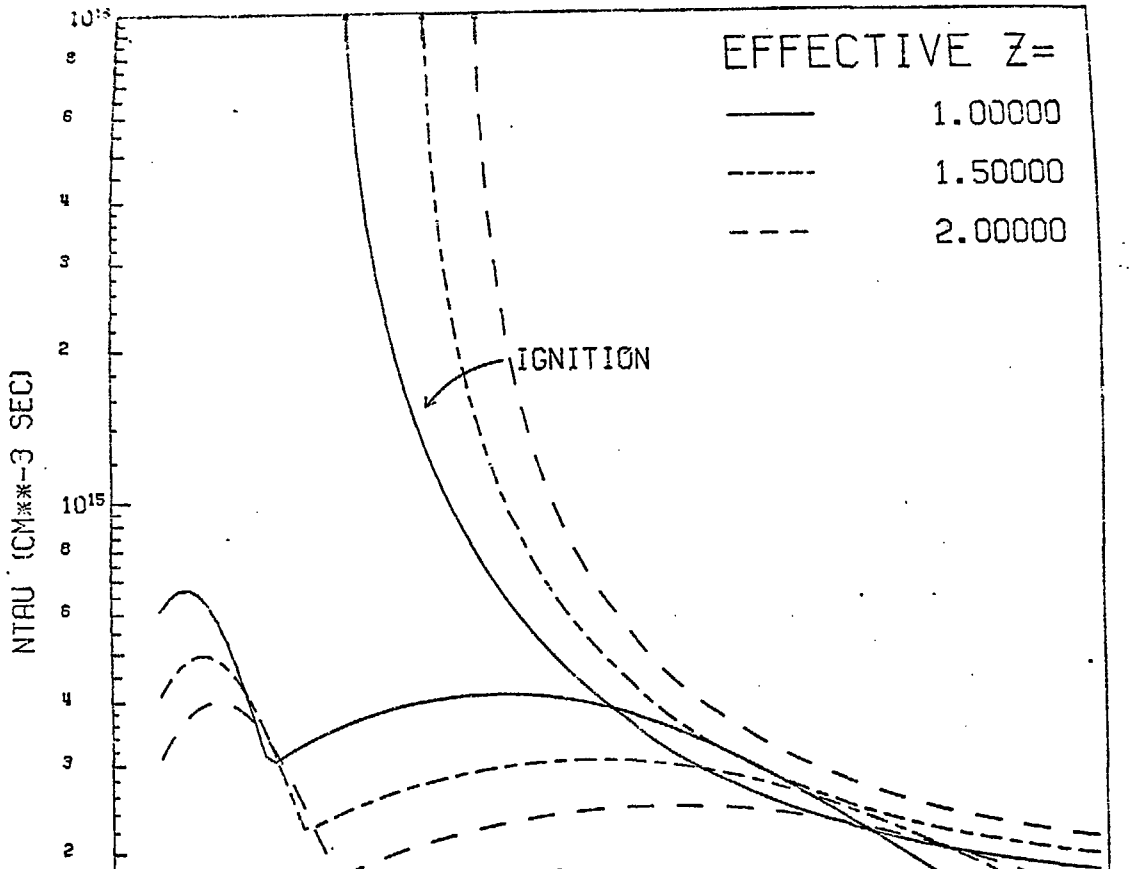

from.

Figure 4.

ORNL-DWG 76-10857

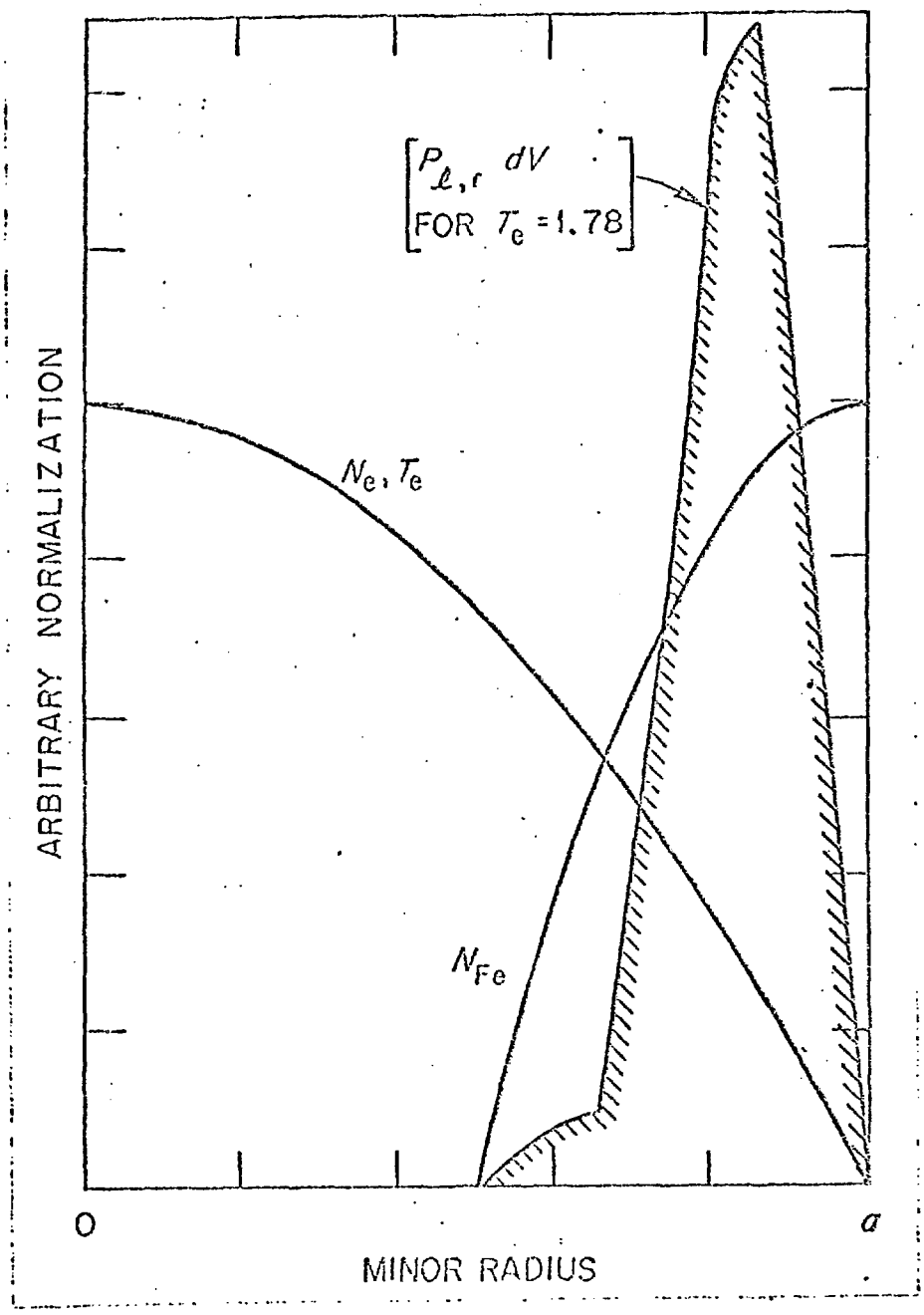

Fig. 3[illegible]. Line and recombination radiation losses (integrated over θ and φ) vs r.

Figure 5

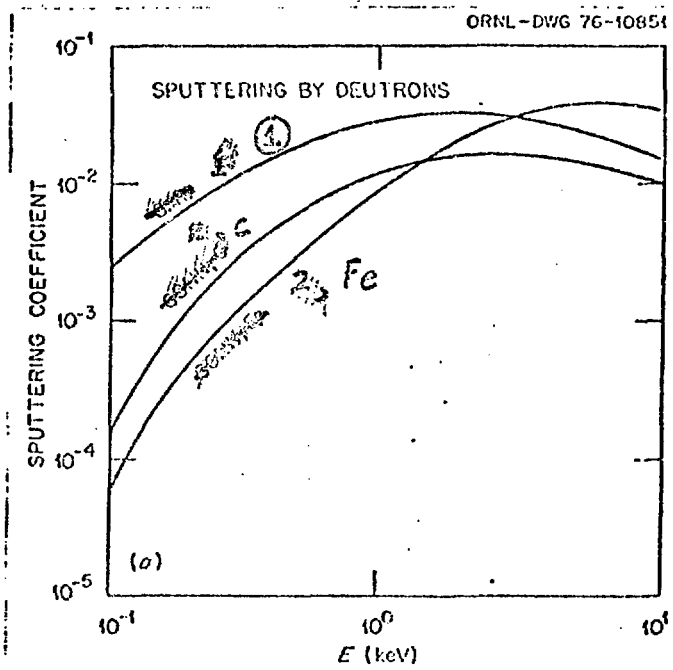
ORNL-DWG 76-10851
SPUTTERING BY DEUTRONS
SPUTTERING COEFFICIENT
10^{-1}
10^{-2}
10^{-3}
10^{-4}
10^{-5}
(a)
10^{-1}
10^{0}
10^{1}
E (keV)
Fe

Figure 6

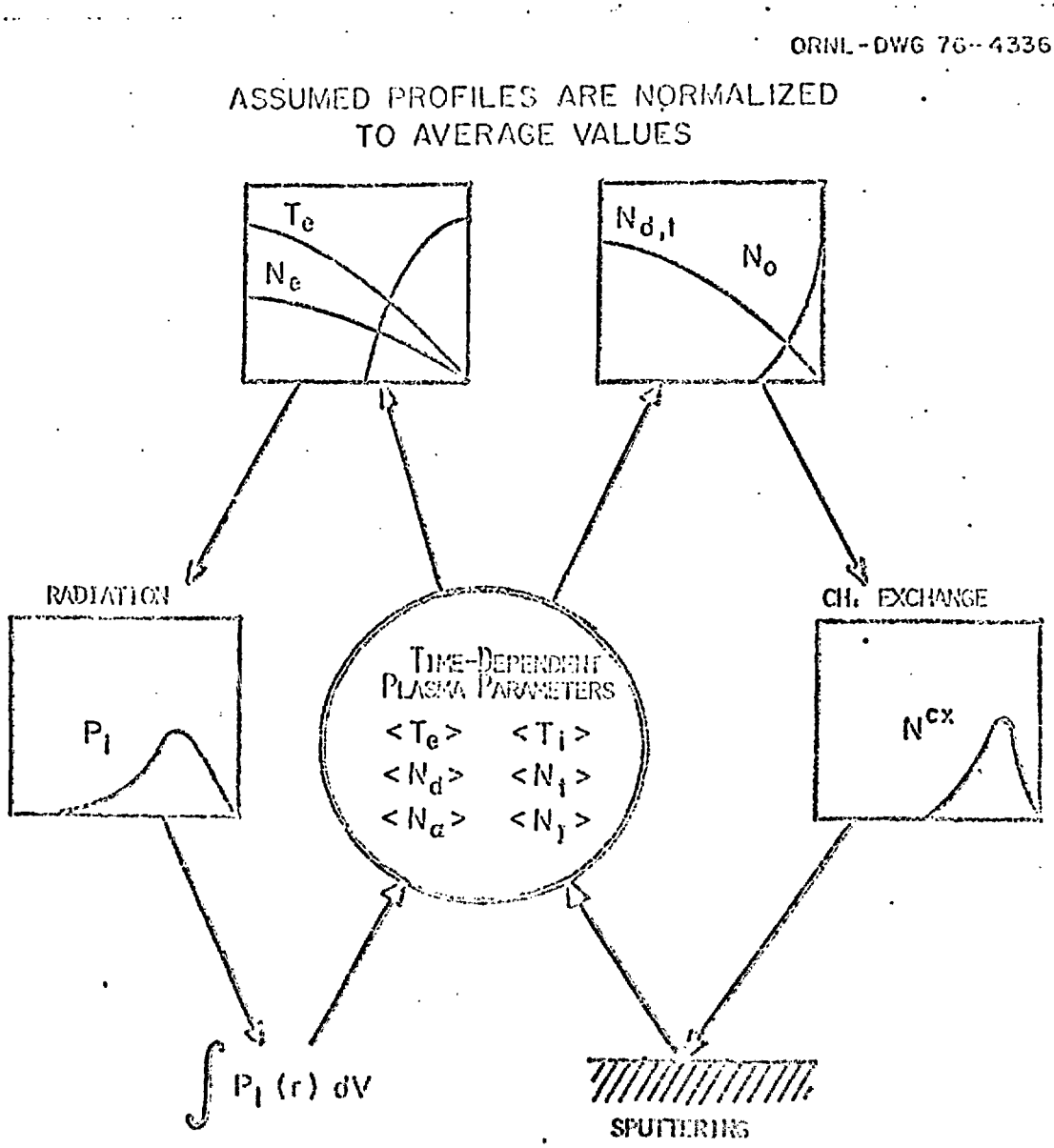

Fig. 3.3. - Incorporation of sputtering and impurity effects in the plasma simulation model.

Figure 7

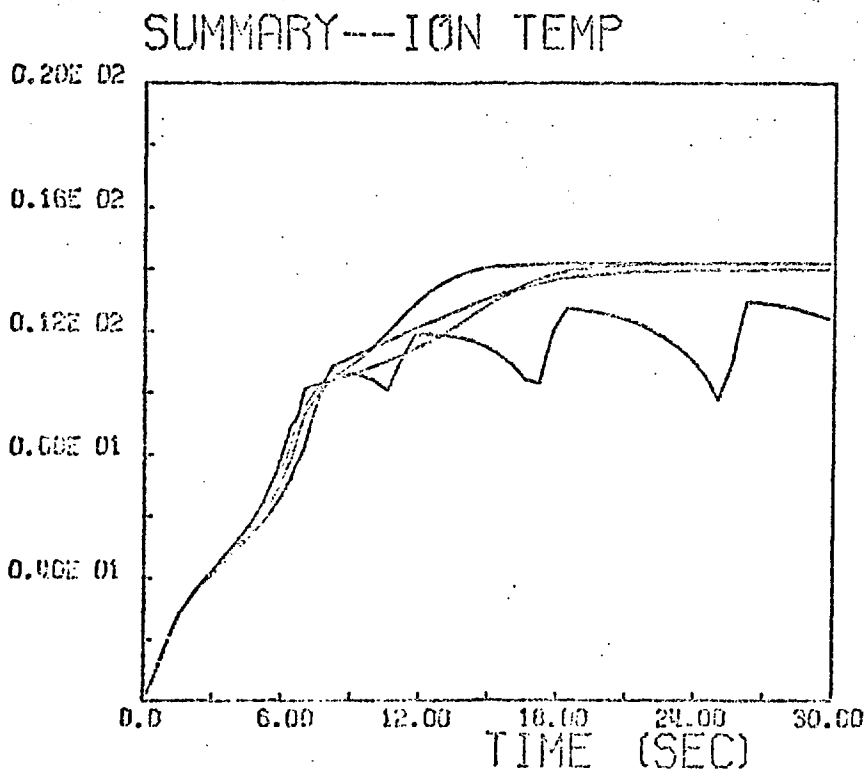
SUMMARY---IØN TEMP
0.20E 02
0.16E 02
0.12E 02
0.08E 01
0.04E 01
0.0
6.00
12.00
18.00
24.00
30.00
TIME (SEC)

Figure 8

THE EFFECT OF DEUTERON ENERGY ON PENETRATION FOR NEAR PERPENDICULAR INJECTION

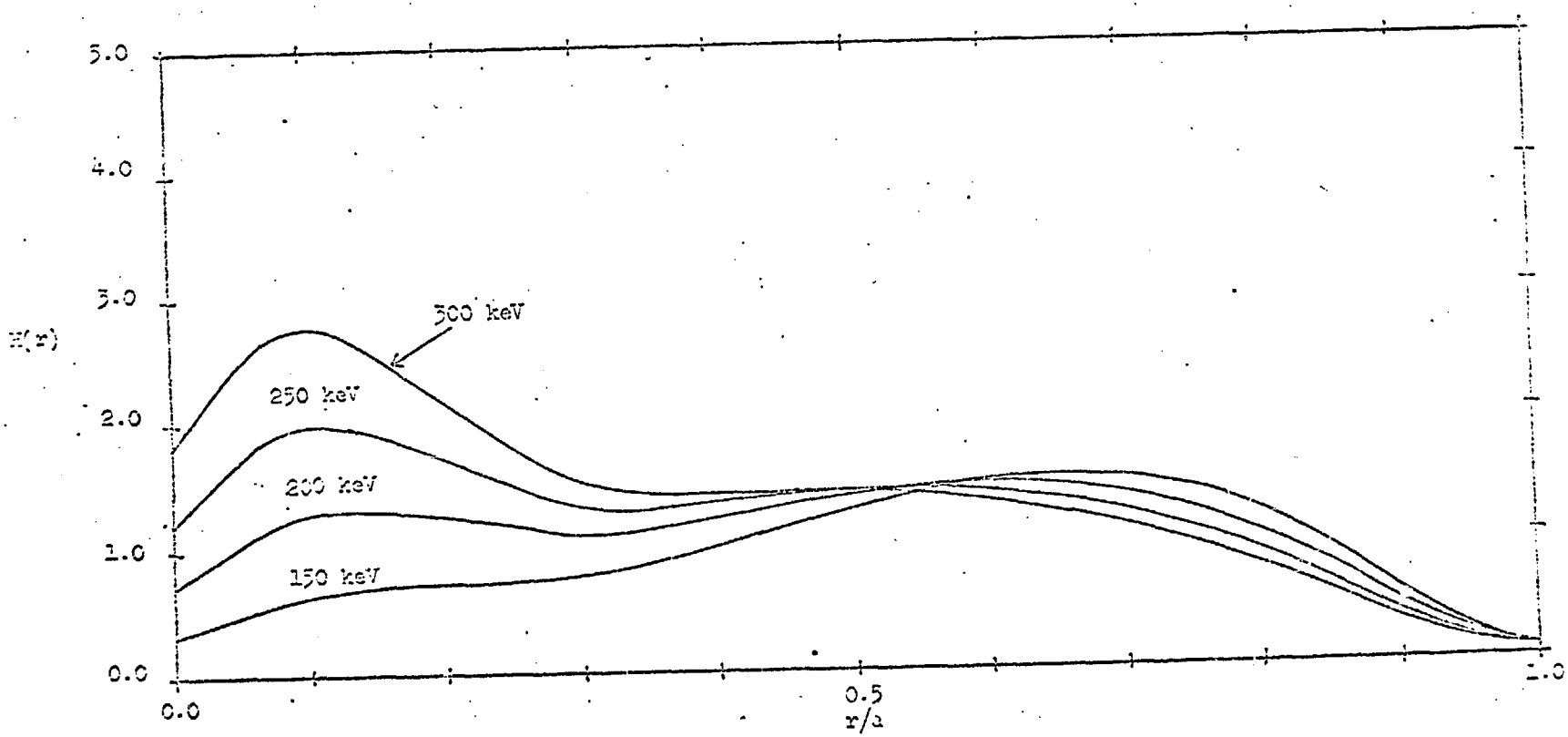

FIGURE ONE.

Figure 9

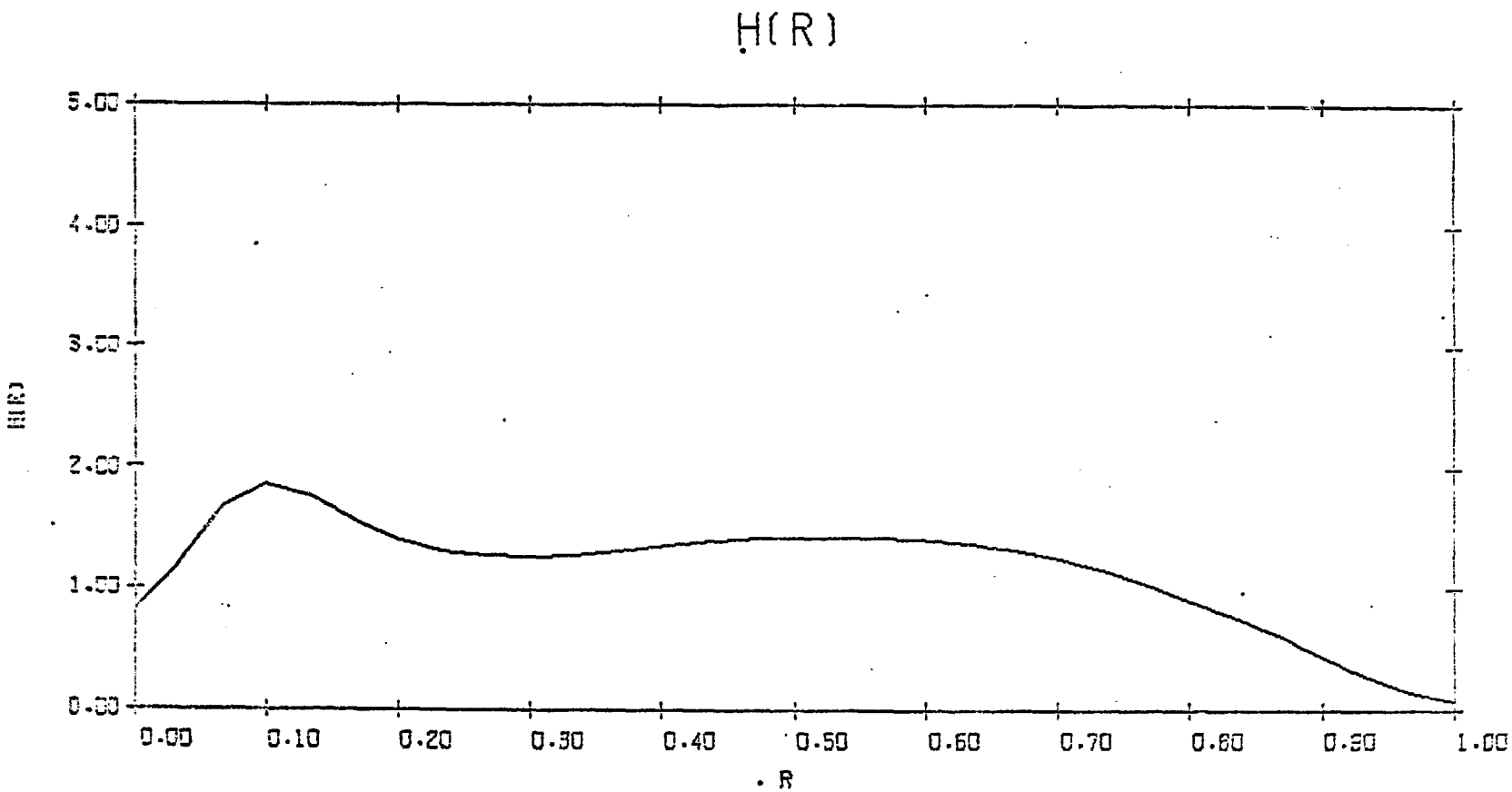
H(R)
5.00
4.00
3.00
2.00
1.00
0.00
H(R)
0.00
0.10
0.20
0.30
0.40
0.50
0.60
0.70
0.80
0.90
1.00
R

Figure 10

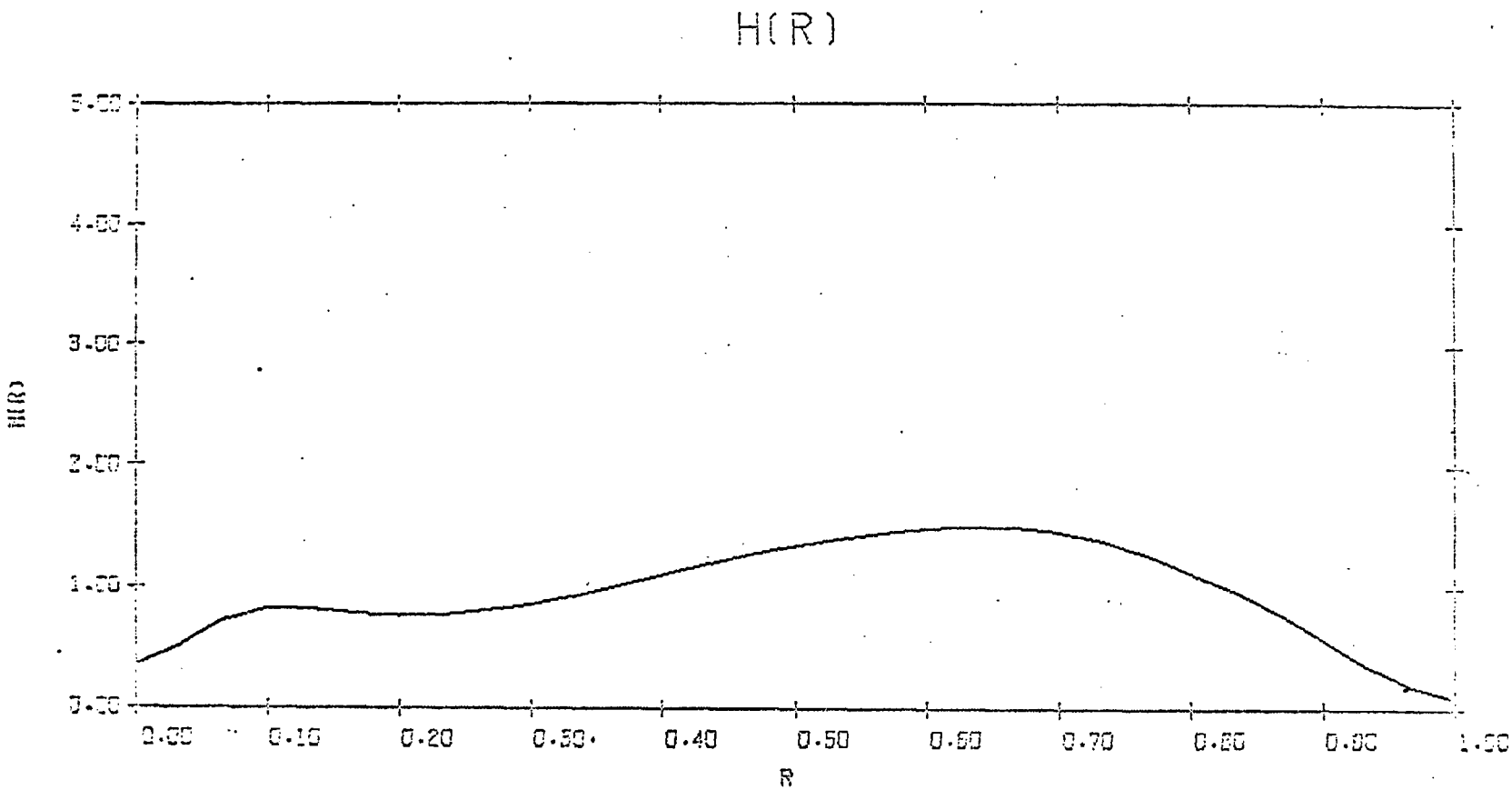
H(R)
5.00
4.00
3.00
2.00
1.00
0.00
H(R)
0.00
0.10
0.20
0.30
0.40
0.50
0.60
0.70
0.80
0.90
1.00
R

Figure 10

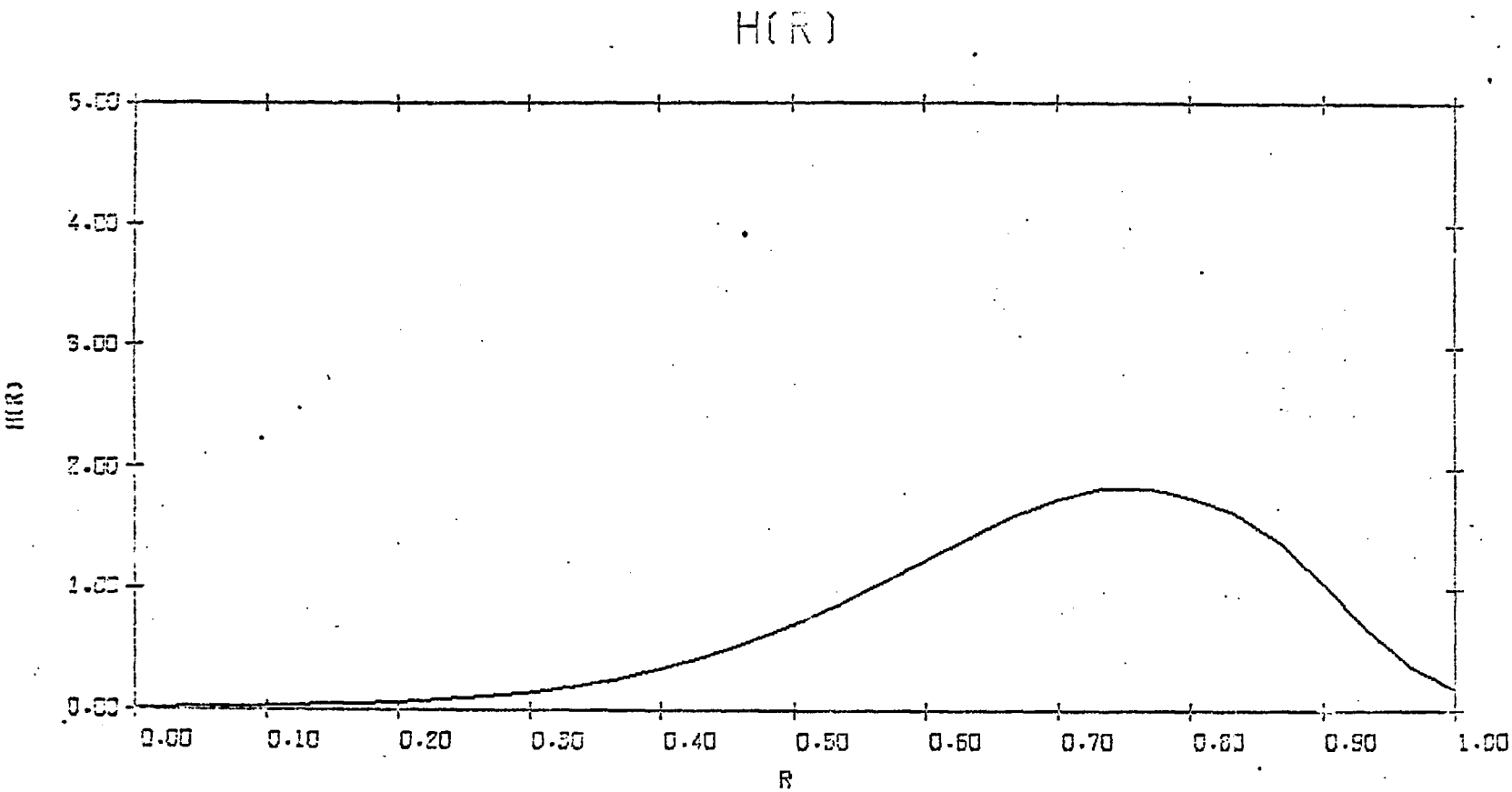
H(R)
5.00
4.00
3.00
2.00
1.00
0.00
H(R)
0.00
0.10
0.20
0.30
0.40
0.50
0.60
0.70
0.80
0.90
1.00
R

Figure 10

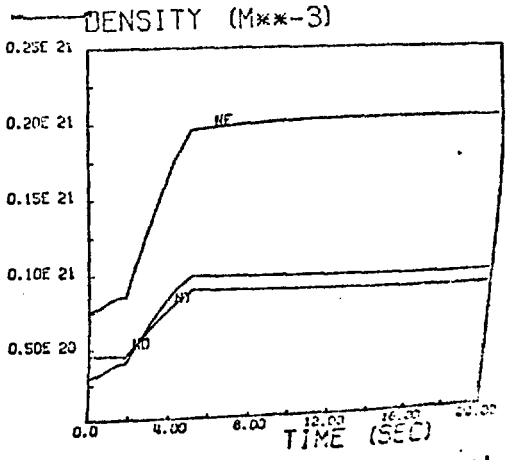

Figure 11

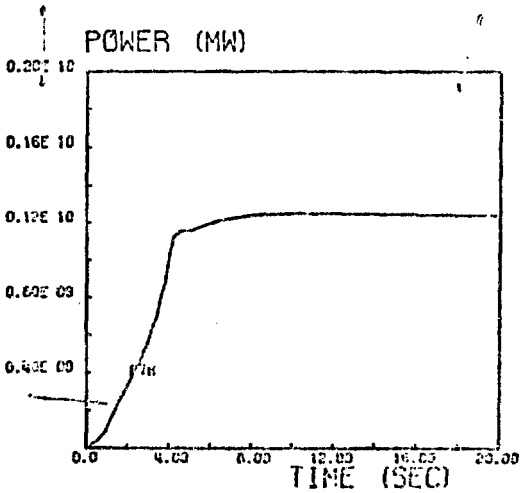

Figure 12